e-Analysis of High-Rise Buildings Subjected to Wind Loads

Dae-Kun Kwon[1]; Tracy Kijewski-Correa[2]; and Ahsan Kareem[3]

Abstract: The NatHaz Aerodynamic Loads Database (NALD) (http://aerodata.ce.nd.edu) introduced in 2000 has served an important first step in establishing an on-line experimental archive of high-frequency base balance (HFBB) data for use in the preliminary design of high-rise buildings subjected to wind loads. As a result, NALD was recently introduced in the Commentary of ASCE 7-05 (C6.5.8) as an alternative means of assessing the dynamic wind load effects on high-rise buildings. This paper presents NALD version 2.0 (v. 2.0), integrating the latest advances in data management and mining for interactive queries of aerodynamic load data and an integrated on-line analysis framework for determining the resulting base moments, displacements, and equivalent static wind loads for survivability and accelerations for serviceability (habitability). The key feature of NALD v. 2.0 is the flexibility its analysis module offers: Users may select not only the data from the on-line NatHaz aerodynamic loads database, but also may input desired power spectral density (PSD) expression or wind tunnel-derived PSD data set obtained from a HFBB experiment for the evaluation of wind load effects on high-rise buildings. Thus, it serves as a stand-alone analysis engine. Examples illustrate the capabilities of NALD v. 2.0 and provide comparisons of response estimates to demonstrate the flexibility of the analysis engine to provide a platform that can be readily expanded and supplemented to yield a comprehensive, simplified, and efficient avenue for e-analysis of high-rise buildings.

Introduction

One of the major challenges in any engineering discipline is the processing and archiving of large quantities of information. This is no exception in the field of structural engineering, where such stores of data include those generated by wind tunnel studies, laboratory experiments, material testing, and even full-scale monitoring. Recent developments in information technology (IT) offer attractive solutions to these challenges, allowing efficient means to collect, store, analyze, manage, and even share large data sets with the worldwide community (Kijewski et al. 2003; Kwon et al. 2005; Fritz and Simiu 2005). Not only do such approaches enable geographically dispersed researchers working on a similar topic to share data and findings, but it also provides a venue in which this information can be disseminated to other members of the design community around the world.

Most codes and standards traditionally have relied on reductive formats and simplifications, which often lead to tables and plots that describe wind loads on structures. The level of accuracy inherent in codification information in this format and the uncertainty associated with interpolation or extrapolation of information may compromise the overall accuracy in code-specified load effects. This has led to database-assisted design procedures, which offer convenient meshing with existing analysis software. Primarily, such databases rely on wind tunnel-derived data, which may be couched in analysis portals to provide desired load effects. One such example is described below.

The NatHaz Aerodynamic Loads Database Version 1.0 (NALD v. 1.0), established in the fall of 2000, is an example of Web-based archiving and distribution of wind tunnel test data for the determination of alongwind, acrosswind, and torsional response (Zhou et al. 2003). This site has served as an important first step in establishing an on-line experimental database for use in the preliminary design of high-rise buildings, which is being extensively consulted by a number of firms (McNamara 2005) and individual researchers (Chan and Chui 2006). This interactive database provides users with the RMS base bending moment coefficients and the nondimensionalized power spectra obtained from high-frequency base balance (HFBB) measurements on rigid building models of various aspect ratios and geometries, exposed to two typical boundary layers. One attractive feature in this package was the use of JAVA-based applets to provide a specific spectral value at a given nondimensional (reduced) frequency, negating potential errors associated with interpolation or curve fitting of spectral data. However, the structure of this prototype site was rather archaic in light of recent advances in data management and mining. This paper discusses the use of advances in the field of information technology to enhance, for the purposes of analysis and design, the accessibility, organization, dissemination, and utility of Web-archived wind tunnel data. The recently redesigned NALD v. 2.0 serves as an example of the application

[1]Postdoctoral Research Associate, Dept. of Civil Engineering and Geological Sciences, Univ. of Notre Dame, Notre Dame, IN 46556. E-mail: dkwon@nd.edu

[2]Rooney Family Assistant Professor, Dept. of Civil Engineering and Geological Sciences, Univ. of Notre Dame, Notre Dame, IN 46556. E-mail: tkijewsk@nd.edu

[3]Robert M. Moran Professor, Dept. of Civil Engineering and Geological Sciences, Univ. of Notre Dame, Notre Dame, IN 46556. E-mail: kareem@nd.edu

of these new technologies. These changes were achieved using a combination of Web-based programming tools and popular engineering software, e.g., Apache Web servers, JAVA/JavaScript, hypertext preprocessors (PHP), structured query language databases (MySQL), and MATLAB. The revised site offers more attractive and user-friendly features to allow not only the retrieval of power spectral values at specific reduced frequencies, but also the on-line determination of resulting base moments, displacements, and equivalent static wind loads (ESWL) for survivability and accelerations for serviceability (habitability) considerations. Thus, in NALD v. 2.0, a dual purpose design aid is introduced: A database-driven Web archive of HFBB data and a stand-alone analysis engine that can be used independently or in tandem for estimating ESWL and building dynamic responses through a user-friendly analysis interface. The latter feature will be particularly useful for those who may not be very familiar with the details of the random vibration-based dynamic analysis procedure generally used in connection with HFBB measurements.

Research to e-Analysis

Measurement of forces using HFBB and synchronous scanning of pressures have become widely accepted techniques for wind tunnel studies of buildings and other structures. The translation of wind tunnel data into ESWL and building response involves a random vibration-based analysis. Most wind tunnel study reports do not provide details of this process with the exception of a generic description in an appendix or a cited reference in the report. This practice has left designers largely in the dark surrounding the theory employed and completely unaware of the many published advances in the procedures for predicting wind-induced response. As such, they are generally not capable of repeating these analyses in house for parametric investigations of period and damping sensitivity that are essential when mitigation of wind-induced motion is required. Instead, design offices often have to engage either a testing laboratory or an external expert to conduct these additional parameter studies. To prevent these analysis procedures from languishing on the library shelves, the NatHaz Modeling and DYNAMO laboratories at the University of Notre Dame have mobilized their technology transfer using information technologies. In this context, this paper chronicles the development of an analysis portal that encompasses necessary features of random vibration analysis to predict building response based on wind tunnel derived data, existing databases, or established expressions for spectral loading, which does not require prior working knowledge of the subject by the user. First, a short history of this development is presented, which is followed by the latest developments.

NatHaz Aerodynamic Loads Database

Aerodynamic loads on buildings may be derived through multiple point synchronous scanning of pressures or by measured forces on the model mounted on a high-frequency base balance. The simultaneously monitored pressure database offers great flexibility in deriving mode generalized loads for buildings with mode shapes that depart from linear or exhibit coupling. However, for tall buildings with dominant resonant response, both the mean and background components can be approximately quantified by modal analysis using integrated wind loads derived from HFBB. The HFBB measurements have been widely recognized for con-

veniently quantifying generalized wind forces on tall buildings with uncoupled mode shapes (Kareem and Cermak 1979; Tschanz and Davenport 1983; Reinhold and Kareem 1986; Boggs and Peterka 1989). The generalized forces are then utilized for estimating building response with given structural characteristics. The HFBB technique generally requires mode shape corrections, which are either based on empirical relationships or analytical formulations derived on the basis of assumed wind loading models (Vickery et al. 1985; Boggs and Peterka 1989; Xu and Kwok 1993; Zhou et al. 2002; Holmes et al. 2003; Chen and Kareem 2004, 2005).

Since its inception a few decades back at Shimizu Corporation's wind tunnel laboratory (Fujii et al. 1986; Kikuchi et al. 1997), synchronous pressure measurements (SPM) on building surfaces have been increasingly implemented in wind tunnel practice. This was largely facilitated by the availability of cheaper electronic pressure sensors and represented an advancement over the covariance-based integration methodology that involved several configurations of limited pressure measurements over a building surface (Kareem 1982). SPM offers the added advantage of providing more accurate estimates of generalized wind loads for buildings with nonlinear mode shapes, as approximate mode shape corrections are not required. Nonetheless, the HFBB maintains its attractiveness in cases where the mode shapes do not depart too far from linear.

Individual researchers (Chen and Kareem 2005; Huang and Chen 2007) and wind tunnel laboratories (Steckley et al. 1992; Ho et al. 1999) have their own favorite analysis format based on either SPM or HFBB. Some groups (Chen and Kareem 2004, 2005) prefer to establish equivalent static wind loads from either SPM or HFBB data for subsequent response analysis, while others directly employ the data for calculating response components (Steckley et al. 1992; Tamura et al. 1996; Ho et al. 1999; Fritz and Simiu 2005).

The NALD consists of results from 162 different tests, derived from nine cross-sectional shapes, three model heights, two exposure categories, and three response directions (alongwind, across-wind, and torsion), as shown by the NALD Web selection menu in Fig. 1. While a detailed description of the test procedures can be found in Kareem (1990), Kijewski and Kareem (1998), and Zhou et al. (2003), a brief summary is now provided. Each of the balsa wood models was tested in a boundary layer wind tunnel with a 3 m (10 ft) × 1.5 m (5 ft) cross section, of 18 m (60 ft) length. The turbulent boundary layers simulated in this study were generated by the natural action of surface roughness added on the tunnel floor and upstream spires. Two typical boundary layers were simulated in this experiment, BL1 (α=0.16, where α=power law exponent of the mean wind velocity profile) and BL2 (α=0.35), similar to the conditions of open [Exposure C in the ASCE 7-05 (ASCE 2005)] and urban [Exposure A in ASCE 7-98 (ASCE 1998)] flow environments, respectively. The output of the sensitive, multicomponent base balance was analyzed using the fast Fourier transform (FFT) to determine the spectral and cross-spectral density functions, which were later nondimensionalized. This analysis was carried out for all 27 building models, in both boundary layers, and at various angles of wind incidence, though only the results from perpendicular approaching winds (zero degree angle of attack) were considered in the NALD v. 1.0. The authors plan to augment the 162 test cases currently housed in the NALD with data for other building shapes and aspect ratios, as they become available from other researchers and/or additional testing.

The reliability of the measured spectra within the NALD has

Fig. 1. NALD data selection menu

been established through verifications against datasets from other wind tunnel experiments. For example, the acrosswind spectra have been compared to a model derived from earlier measurements by Kareem (1990). Results in the torsional direction were also compared to those derived from pneumatic averaging, to overcome the uniform mode shape assumption inherent to the HFBB-derived torsional loads (Kareem 1990). More recently, Zhou et al. (2003) compared the NALD acrosswind loads with the empirical expression suggested by the Architectural Institute of Japan (AIJ 1996; Tamura et al. 1996). In addition, nondimensionalized base moment coefficients were compared to the empirical expressions given by AIJ for acrosswind and torsional directions (Zhou et al. 2003).

Since these previously reported comparisons, a number of new studies concerning HFBB and SPM have been published (Liang et al. 2002, 2004; Cheng and Wang 2004; Gu and Quan 2004; Ha et al. 2004; Lin et al. 2005; Flay and Bhat 2005). In particular, it is worth noting that Lin et al. (2005) have provided an in-depth comparison of the NALD to their HFBB and SPM. They found the NALD to be in close agreement with their studies with the exception of a few cases, stating: "With the linear mode shape assumption . . . integrated simultaneous point pressures and HFBB agree for base force and moment spectra. The [NALD] effectively provides the base moment spectra for preliminary design and can be expanded on the Internet by the dataset here and by the other experimental results in the future" (Lin et al. 2005). This speaks not only to the reliability of the NALD, but also the robustness of its framework for future expansion. The examples

in this paper offer additional verification of NALD against selected major studies, though these are by no means exhaustive or meant to serve as a systematic comparison of HFBB data from different laboratories, codes, and standards.

Overview of NALD v. 2.0: from Theory to Practice

Theoretical Background of NALD v. 2.0

To account for the gustiness of turbulent boundary-layer winds on structures, most international codes and standards including ASCE 7 have adopted the concept of gust loading factor (GLF), which was first introduced by Davenport (1967) based on statistical theory of buffeting. This traditional GLF is based on the ratio of the maximum structural displacement to the mean displacement (Davenport 1967; Solari and Kareem 1998). Although the traditional GLF ensures an accurate estimation of the displacement response, it may fall short in providing a reliable estimate of other response components. To overcome this shortcoming, Zhou and Kareem (2001) proposed a new GLF format that is based on the ratio between the maximum base bending moment and the mean obtained from HFBB experiments, rather than the displacements utilized in the conventional approach.

This new GLF format associated with base moments has been introduced in ASCE 7-05 (ASCE 2005) as well as the AIJ (2004) *Recommendations for Loads on Buildings*. Using the aerodynamic base bending moment or base torque as the input, the

wind-induced response of a building can be computed using random vibration analysis as detailed in Zhou and Kareem (2001). Utilizing the base bending moment, NALD v. 2.0 assists in evaluating the equivalent static wind loads and attendant response components. Due to relatively less sensitivity of the base moment to mode shapes, the mode shape correction may not be necessary in this approach. Application of this framework for the alongwind response has proven effective in recasting the traditional gust loading factor approach into a new format. This procedure has been extended to the acrosswind and torsional response in a 3D gust loading factor approach (Zhou and Kareem 2001; Kareem and Zhou 2003).

Although the theoretical background adopted in NALD v. 2.0 has been introduced in Zhou and Kareem (2001), Zhou et al. (2003), Kareem and Zhou (2003), and Tamura et al. (2005), it is briefly described here for completeness. Assuming the response is a stationary Gaussian process, the expected maximum base bending moment response $(\hat{M})$ in the alongwind and acrosswind directions or the base torque response can be expressed in the following form:

$$\hat{M} = \bar{M} + g \times \sigma_M \approx \bar{M} + \sqrt{M_B^2 + M_R^2} = \bar{M} + \sqrt{(g_B \times \sigma_{CM} \times \bar{M}')^2 + \left(g_R \times \sigma_{CM} \times \bar{M}' \times \sqrt{\frac{\pi}{4\zeta_1} C_M(f_{r1})}\right)^2} \quad (1)$$

where $\bar{M}$=mean moment; M_B, M_R=background and resonant base moment or torque components, respectively; g, g_B, g_R=peak factors for total, background, and resonant moments, respectively; σ_M, σ_{CM}=RMS of the fluctuating base moment/torque response and base moment/torque response coefficient $(=\sigma_M/\bar{M}')$; $\bar{M}'$=reference moment or torque depending on response component; ζ_1=building damping ratio in the first mode; $C_M(f_{r1})$=nondimensional moment coefficient at f_{r1} $(=f_{r1} \times S_M(f_{r1})/\sigma_M^2)$; f_{r1}=reduced frequency according to f_1 $(=f_1 B/\bar{U}_H)$; f_1=natural frequency of building in the direction of motion; $S_M(f)$=PSD of the fluctuating base moment or torque response; f=frequency [Hz]; $\bar{U}_H$=mean wind velocity evaluated at building height H. In addition, since σ_{CM} and $C_M(f_{r1})$ are obtained from the HFBB experiment, the mean, background, and resonant base moments can be computed in the alongwind, acrosswind, and torsional directions using respective building properties. This has led to the introduction of a 3D GLF approach to facilitate evaluation of response in three directions (Kareem and Zhou 2003). The gust loading factor G_M associated with base moment can be described as the following form:

$$G_M = \hat{M}/\bar{M}' = \bar{G} + \sqrt{G_{MB}^2 + G_{MR}^2} \quad (2)$$

Thus, mean $(\bar{G})$, background (G_{MB}), and resonant (G_{MR}) GLF can be easily derived by comparing Eq. (2) to Eq. (1) (Kareem and Zhou 2003). Using Eqs. (1) and (2), the ESWL on a building in the alongwind, acrosswind, and torsional directions can be computed by distributing the base moments to each floor akin to the manner in which base shear is distributed in earthquake engineering. The mean base moment $(\bar{M})$ has a relationship with the mean component of the ESWL as follows:

$$\bar{M} = \int_0^z \bar{P}(z) \times z \, dz \quad (3)$$

where mean component of the ESWL $(\bar{P})$ is

$$\bar{P}(z) = \frac{1}{2}\rho \bar{U}_H^2 \left(\frac{z}{H}\right)^{2\alpha} BC_D \Delta H = \bar{M}\frac{2+2\alpha}{H^2}\left(\frac{z}{H}\right)^{2\alpha}\Delta H \quad (4)$$

Next, the background component for the alongwind and acrosswind responses can be obtained by using the background GLF as follows:

$$P_{B(D,L)}(z) = G_{MB(D,L)} \times \bar{P}(z) = M_{B(D,L)}\frac{2+2\alpha}{H^2}\left(\frac{z}{H}\right)^{2\alpha}\Delta H \quad (5)$$

Similarly, the background component for the torsional response $(P_{B(T)})$ is expressed as

$$P_{B(T)}(z) = G_{MB(T)} \times \bar{P}(z) = M_{B(T)}\frac{1+2\alpha}{H}\left(\frac{z}{H}\right)^{2\alpha}\Delta H \quad (6)$$

where subscripts B, D, L, and T=background, alongwind, acrosswind, and torsional components; ρ=air density; z=elevation above the ground; B=building width; C_D=drag force coefficient; ΔH=floor-to-floor height of building; α=exponent of mean wind speed profile defined in ASCE 7.

For the resonant components, the ESWL in sway modes is given by

$$P_{R(D,L)}(z) = M_{R(D,L)}\frac{m(z)\varphi_{1(D,L)}}{\sum m(z)z\varphi_{1(D,L)}} \quad (7)$$

and in the torsional mode

$$P_{R(T)}(z) = M_{R(T)}\frac{I(z)\varphi_{1(T)}}{\sum I(z)\varphi_{1(T)}} \quad (8)$$

where subscript R=resonant component; $m(z)$=mass per unit height; φ_1=fundamental mode shape in the direction of motion $(=(z/H)^\beta)$; β=mode shape exponent in the direction of motion, e.g., linear mode shape if $\beta = 1$; $I(z)$=mass moment of inertia per unit height $(=m(z) \times \gamma^2)$; γ=radius of gyration.

For the acceleration response, only the resonant component is of interest. The peak accelerations for the three principle directions of motion, i.e., alongwind, acrosswind, and torsion, can be obtained by the following equations:

- Alongwind and acrosswind

$$\ddot{Y}_{\text{Peak}(D,L)}(z) = \frac{P^*_{R(D,L)}}{K^*_{(D,L)}} \varphi_{1(D,L)} \times (2\pi f_1)^2$$

$$= \frac{\displaystyle\int_0^H P_{R(D,L)}(z)\varphi_{1(D,L)}dz}{\displaystyle\int_0^H m(z)\varphi^2_{1(D,L)}dz} \varphi_{1(D,L)} \qquad (9)$$

- Torsion

$$\ddot{Y}_{\text{Peak}(T)}(z) = \frac{P^*_{R(T)}}{K^*_{(T)}} \varphi_{1(T)} \times (2\pi f_1)^2 = \frac{\displaystyle\int_0^H P_{R(T)}(z)\varphi_{1(T)}dz}{\displaystyle\int_0^H I(z)\varphi^2_{1(T)}dz} \varphi_{1(T)}$$

$$(10)$$

where P^*=generalized force; K^*=generalized stiffness. The resulting RMS acceleration can then be determined by dividing the peak accelerations by the resonant peak factor g_R. Note that the angular accelerations in torsion may be resolved into the resultant alongwind and acrosswind components at the corner of the building, and these lateral accelerations induced by torsion can be combined with those generated by the sway motions to obtain the total lateral accelerations at the corner by the square root of the sum of the squares (SRSS) or complete quadratic combination (CQC) (Zhou et al. 2003; Chen and Kareem 2004, 2005).

The displacement response calculation can be computed by a modal analysis procedure. Assuming that building mass is uniformly distributed along the height, i.e., mass per unit height $[m(z)]$ being a constant value (m), the mean and maximum displacements in the alongwind can be computed by the following expressions:

$$Y_{\text{mean}(D)}(z) = \frac{P^*_{\text{mean}(D)}}{K^*_{(D)}} \varphi_1 = \frac{(2\beta+1)\bar{M}}{mH^2(2\pi f_1)^2}\left(\frac{z}{H}\right)^\beta$$

$$Y_{\text{max}(D)}(z) = G_M \times Y_{\text{mean}(D)}(z) \qquad (11)$$

Similarly, the maximum displacement in the acrosswind direction is computed by only including background and resonant displacements, since there is no mean displacement in this direction

$$Y_{B(L)}(z) = \frac{P^*_{B(L)}}{K^*_{(L)}} \varphi_1 = \frac{M_{B(L)}(2\beta+1)(2+2\alpha)}{mH^2(2\pi f_1)^2(2\alpha+\beta+1)}\left(\frac{z}{H}\right)^\beta$$

$$Y_{R(L)}(z) = \frac{P^*_{R(L)}}{K^*_{(L)}} \varphi_1 = \frac{M_{R(L)}(\beta+2)}{mH^2(2\pi f_1)^2}\left(\frac{z}{H}\right)^\beta$$

$$Y_{\text{max}(L)}(z) = \sqrt{Y^2_{B(L)}(z) + Y^2_{R(L)}(z)} \qquad (12)$$

Alternatively, if the RMS moment coefficient ($\sigma_{\text{CM}(L)}$) and nondimensional moment coefficient $[C_{M(L)}(f)]$ in the acrosswind direction, which can be obtained from NALD as well, are known for given building properties, the background and resonant displacements in the acrosswind direction can be obtained from the following expressions in which Eq. (12) is expanded by using $M_{B(L)}$ and $M_{R(L)}$ [see Eq. (1)]:

$$Y_{B(L)}(z) = \frac{1}{2}\rho \times \bar{U}_H^2 \times D \times g_B \times \sigma_{\text{CM}(L)}$$

$$\times \frac{(2+2\alpha)(2\beta+1)}{m(2\alpha+\beta+1)(2\pi f_1)^2} \times \left(\frac{z}{H}\right)^\beta$$

$$Y_{R(L)}(z) = \frac{1}{2}\rho \times \bar{U}_H^2 \times D \times g_{R(L)} \times \sigma_{\text{CM}(L)}$$

$$\times \sqrt{\frac{\pi}{4s_1}C_{M(L)}(f_{r1})} \times \frac{(\beta+2)}{m(2\pi f_1)^2} \times \left(\frac{z}{H}\right)^\beta \qquad (13)$$

Note that all parameters in Eqs. (11)–(13) are related to acrosswind properties, e.g., f_1 here is natural frequency of building in the acrosswind direction. Note that the displacement response is dictated by 50-year wind speeds, as this is the mean recurrence interval (MRI) for base moments and the ESWL (survivability design), while the acceleration response is governed by the 10-year wind speed (serviceability design).

Database-Enabled Selection

NALD v. 1.0 (Zhou et al. 2003) provided users with wind tunnel measurements of RMS base moment coefficients and the nondimensional power spectral values requisite for the above response calculations for the 162 tests discussed previously. Upon entering the database, the user stepped through a series of hypertext markup language (HTML) links to identify the data of interest. Once the desired test case and response component were selected, a JAVA applet retrieved the exact nondimensionalized power spectral value corresponding to a user-specified reduced frequency. This automated process negates potential human errors that result from picking off values from hardcopy spectra and eliminates the uncertainty associated with curve-fit expressions that tend to generalize spectral features. However, since the NALD v. 1.0 could not support structured query language (SQL), the architecture associated with this prototype involved an expansive hierarchy of directories with duplicate HTML files, requiring the user to step through a sequence of at least five Web pages to reach the desired JAVA applet.

To reduce the redundancy in the architecture, several Web-based tools were utilized in NALD v. 2.0, now hosted by a dedicated Apache Web server available to the public at http://aerodata.ce.nd.edu. This hardware change now permits the use of PHP, a kind of common gateway interface (CGI) language, and MySQL for a database-oriented query to specify the desired test data, replacing the archaic and sequential HTML structure of the original site. This speeds the retrieval time and dramatically reduces the number of HTML files, directories, and total file sizes by eliminating unnecessary redundancies on the server. It also provides inherent scalability so the data archives can be readily expanded. The new user-friendly interface was shown in Fig. 1 and allows the selection of a desired test case in only one step, which is then followed by the launch of the appropriate JAVA applet from NALD v. 1.0 (Zhou et al. 2003), with the option for downloading data for further off-line analysis. It is worth noting that NALD v. 2.0 has been introduced in the commentary of ASCE 7-05 [C6.5.8] (ASCE 2005) as an alternative means to assess the dynamic wind-induced loads on typical isolated buildings in the preliminary design stages.
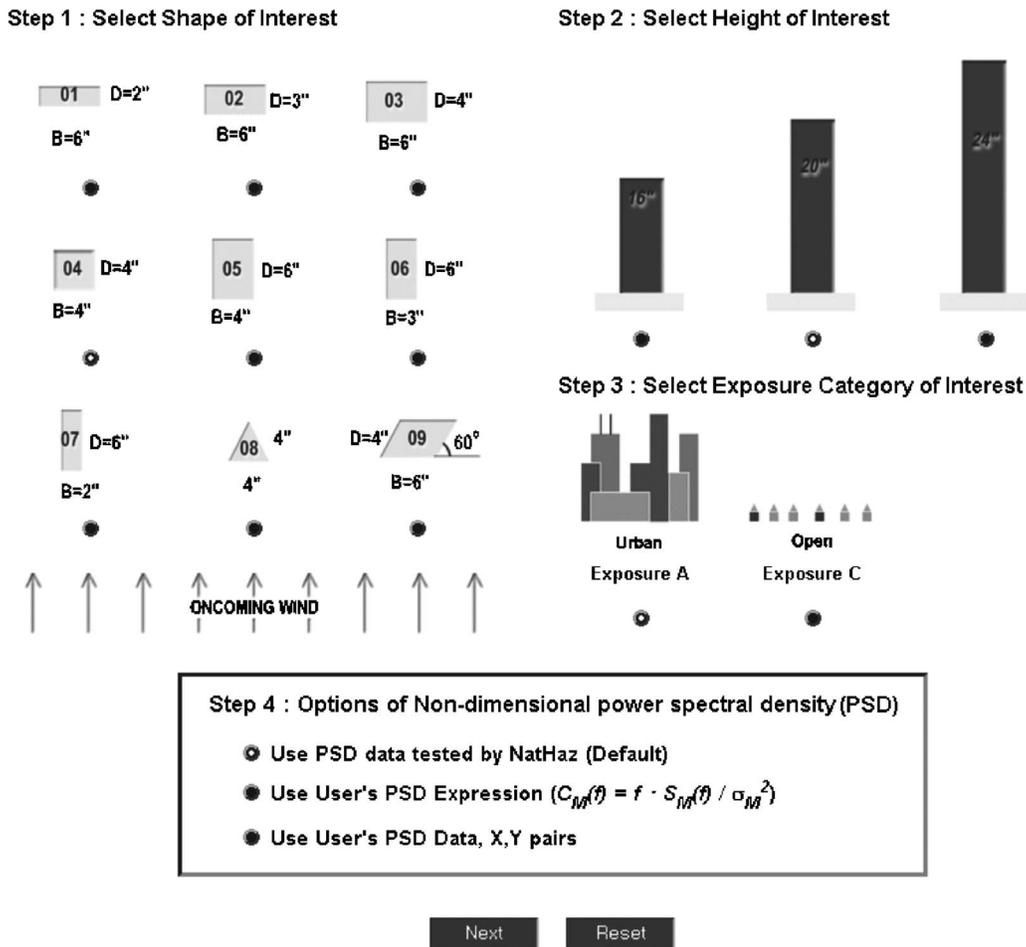
Fig. 2. NALD v. 2.0 data selection menu for on-line analysis, including PSD option

---

On-Line Analysis of Wind Loads and Response

In NALD v. 1.0, users would retrieve relevant spectral properties for a given test case and then manually perform off-line calculations to obtain the building base bending moments, ESWL, and accelerations based on the equations introduced previously (Zhou et al. 2003). To minimize the calculations required on the part of the end user, an on-line analysis module was developed utilizing the theory presented in the previous section to supplement the existing JAVA interface and provide these and other response quantities automatically.

The new user interface developed for on-line analysis is shown in Fig. 2. It is similar to the reorganized selection menu (Fig. 1), but with additional options for specifying the input power spectral density (PSD). At present, three user options are available for prescribing a PSD for the analysis: PSD data from the NALD (default option), a user-specified PSD (curve-fitted or analytical expression) or user-supplied PSD data (X, Y data pairs). The user selections are handled by a combination of PHP and MySQL as inputs for the next stage in the process. After selecting these basic inputs, the module requests additional inputs for the full-scale system, including cross-sectional dimensions, height, exposure

category, and fundamental dynamic characteristics (Fig. 3). Either metric (SI) or English units may be specified for the structural inputs and calculated outputs. In addition, an on-line calculator is provided for user-friendly unit conversion (Fig. 4). It should be noted that ASCE 7 recommends a 50-year mean recurrence wind that is used in survivability design, e.g., ESWL evaluation, whereas, in serviceability design, a building's acceleration is generally based on a 10-year mean recurrence wind. Thus, it is required to include a MRI factor to convert 50-year winds into 10-year winds for serviceability design. For convenience, wind speeds for both survivability (50-year MRI) and serviceability (10-year MRI) in the exposure of interest are calculated on-the-fly in NALD v. 2.0 (Fig. 5) based on the relationships in ASCE 7-05 (ASCE 2005) utilizing the user-specified 3-sec gust 50-year reference wind speed (U_{10}) in open terrain (Fig. 3). Nondimensional spectral values $[C_M(f)]$ are then calculated on-the-fly for all directions and mean recurrence intervals (Fig. 5). Thus, the JAVA applets are no longer required in this new on-line analysis module.

MATLAB provides an attractive programming framework for more complicated computations and can be easily extended to

Step 5 : Please select options and fill out input values.   On-line Unit Converter

■ Please select the unit of input values (default : Metric)
 If user would like to see English unit output, please select checkbox (default : Metric)

  ⦿ Metric(SI) unit [kg, m, m/s]   ⦿ English unit [lb, ft, mph]   ■ Output : English unit

■ Building width(B), depth(D) and height(H)

 B [m, ft] : ⬛   D [m, ft] : ⬛   H [m, ft] : ⬛

■ Natural frequencies of building for three directions; alongwind(f_x), acrosswind(f_y) and torsional(f_z).

 f_x [Hz] : ⬛ f_y [Hz] : ⬛ f_z [Hz] : ⬛

■ Mode shape exponents(β) for three directions, $(z/H)^\beta$ (default : linear mode shape, β=1.0)

 alongwind(β_1) : 1.0   acrosswind(β_2) : 1.0   torsional(β_3) : 1.0

■ Bulk density(ρ_B), average radius of gyration(γ) and damping ratio(ζ) of building

 ρ_B [kg/m^3, lb/ft^3] : ⬛ γ [m, ft] : ⬛ ζ : ⬛

■ Floor-to-floor height of building(ΔH), Air density(ρ_A), drag force coefficient(C_D)

 ΔH [m, ft] : ⬛ ρ_A [kg/m^3, lb/ft^3] : ⬛ C_D : ⬛

■ From ASCE standard 7-98 (Fig. 6-1)
 3-second basic wind speed(U_{10}), file name(.dat) for wind force output (default : w_force),
 select checkbox if this building is located in Alaska

 U_{10} [m/s, mph] : ⬛   file name : w_for   ■ Alaska

■ User selected to use NatHaz PSD data.

[Submit]   [Reset]

Fig. 3. Interface for user-supplied structural inputs

On-line Unit Converter

■ **Length**

  [   ] [m ▼]

0	m	0	cm
0	ft	0	in
0	yd	0	mile

■ **Velocity**

  [   ] [m/s ▼]

0	m/s	0	cm/s
0	ft/s	0	in/s
0	km/hr	0	mph

■ **Density**

  [   ] [kg/m³ ▼]

0	kg/m^3	0	g/cm^3
0	lb/ft^3	0	lb/in^3

■ **Acceleration**

  [   ] [m/s² ▼]

0	m/s^2	0	ft/s^2
0	milli-g	0	gal

■ **Force**

  [   ] [N ▼]

0	N	0	kgf
0	lbf	0	kips

■ **Moment**

  [   ] [N·m ▼]

0	N·m	0	kgf·m
0	lbf·ft	0	kips·ft

Fig. 4. On-line unit conversion module

Survivability design (50-year return period) : U_H = 51.30 m/s
Serviceability design (10-year return period) : U_H = 37.96 m/s

■ RMS base moment coefficients(σ_{CM}), reduced frequencies($f_1 \cdot B / U_H$) and non-dimensional moment coefficients($C_M (f_1)$)

	σ_{CM}	$f_1 \cdot B / U_H$		$C_M (f_1)$	
		50-year	10-year	50-year	10-year
Alongwind	0.109	0.156	0.211	0.048	0.040
Acrosswind	0.133	0.156	0.211	0.192	0.073
Torsional	0.044	0.273	0.369	0.060	0.039

Fig. 5. NALD v. 2.0 output from on-the-fly calculation of wind speeds and nondimensional moment coefficients

more sophisticated numerical calculations due to many predefined function capabilities. For these reasons, MATLAB (version 6.5, R13) is used as the computational framework for this study, and the MATLAB Web server tool is internally utilized to supply user inputs to the server-side MATLAB analysis. A MATLAB code, running on the NALD server, determines the base moment/torque, the structural displacements and accelerations, in addition, to the ESWL for the mean, background, and the resonant components. The following quantities are then displayed on the Web portal: Nondimensional spectral base moment (Fig. 6), RMS base moment coefficient, nondimensional moment coefficient, base moment and the maximum lateral displacements for survivability design, 10-year RMS and peak lateral accelerations, corresponding lateral accelerations induced by torsion, and total lateral accelerations at the corner. All displacements and accelerations are calculated at the roof level. All these quantities, i.e., base bending moments, displacements, and accelerations are displayed for each of the three response components (Fig. 7). Finally, a plot of the mean, background, and resonant components of the ESWL on the building are displayed for the end user, as shown in Fig. 8. An option is also available to download this information as a text file for further off-line analysis and possible application to an existing structural finite element model or a spreadsheet-based building analysis. As such, the NALD v. 2.0 can also be used to express wind loads, i.e., the ESWL, in three directions in terms of 3D gust loading factors, akin to the alongwind GLF (Kareem and Zhou 2003; Tamura et al. 2005).

■ Non-dimensional PSD for alongwind, acrosswind and torsional ($C_M(f) = f \cdot S_M(f) / \sigma_M^2$)
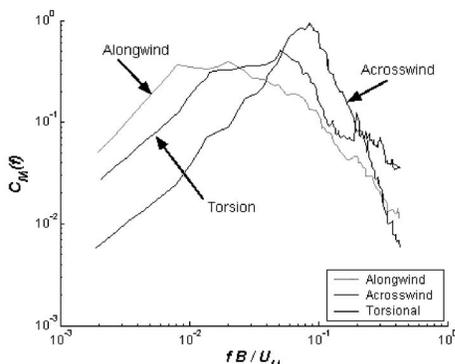
Fig. 6. Nondimensional base moment spectra display

■ Survivability Design (50-year wind) : Base moments

	Base Moment (10^6 kN-m)			
	$\bar{M}$	$\hat{M}_B$	$\hat{M}_R$	$\hat{M}$
Alongwind	1.2828	0.9734	1.4828	3.0566
Acrosswind	-	1.1899	3.6403	3.8298
Torsional	-	0.0784	0.1386	0.1592

■ Survivability Design (50-year wind) : Maximum Displacements

	Maximum Displacements at roof
Alongwind	0.363 m
Acrosswind	0.455 m

■ Serviceability Design (10-year wind) : Peak and RMS Accelerations

	Peak Accelerations at roof	
Alongwind	14.19 $milli$-g	
Acrosswind	23.50 $milli$-g	
Lateral Accelerations at Corner Induced by Torsion	0.00476 rad/s^2	Alongwind component : 9.70 $milli$-g
		Acrosswind component : 9.70 $milli$-g
Total Lateral Accelerations at Corner	Alongwind component : 17.19 $milli$-g Acrosswind component : 25.43 $milli$-g	

	RMS Accelerations at roof	
Alongwind	3.75 $milli$-g	
Acrosswind	6.21 $milli$-g	
Lateral Accelerations at Corner Induced by Torsion	0.00121 rad/s^2	Alongwind component : 2.47 $milli$-g
		Acrosswind component : 2.47 $milli$-g
Total Lateral Accelerations at Corner	Alongwind component : 4.49 $milli$-g Acrosswind component : 6.68 $milli$-g	

Fig. 7. Display of on-the-fly calculated survivability and serviceability values

The architecture of NALD v. 2.0 and the role of various Web-based tools such as HTML/JAVA Script and PHP are summarized in Fig. 9. It is basically operated by Apache Web server with two main processes, i.e., external process and internal process. The external process includes user-friendly interfaces for the selection of a desired analysis case in Fig. 2 (interface 1), additional interfaces for design inputs such as structural parameters of building in Fig. 3 (interface 2), and display of analysis results for the user-specified building. On the other hand, the internal processes are server-side operations involving MySQL for database operations and MATLAB Web servers for the computational schemes implicitly utilized in NALD v. 2.0. The MySQL database server handles data transmissions between interfaces and if necessary, transmits information stored in the database. The MATLAB Web server functions as a numerical analysis engine for on-the-fly calculations, as well as serving as the nexus between interface 2 and the design results. The on-line analysis module performs the requisite calculations and then generates meaningful figures such as the nondimensional PSD and the ESWL, as well as the ESWL text file.

It should again be emphasized that one unique feature provided by this on-line analysis module is the user's nondimensional PSD options. As mentioned earlier, NALD v. 2.0 provides the user with three PSD options. Thus, the user can utilize not

A: mean component

B: alongwind background component

C: alongwind resonant component

D: acrosswind background component

E: acrosswind resonant component

F: torsional background component

G: torsional resonant component
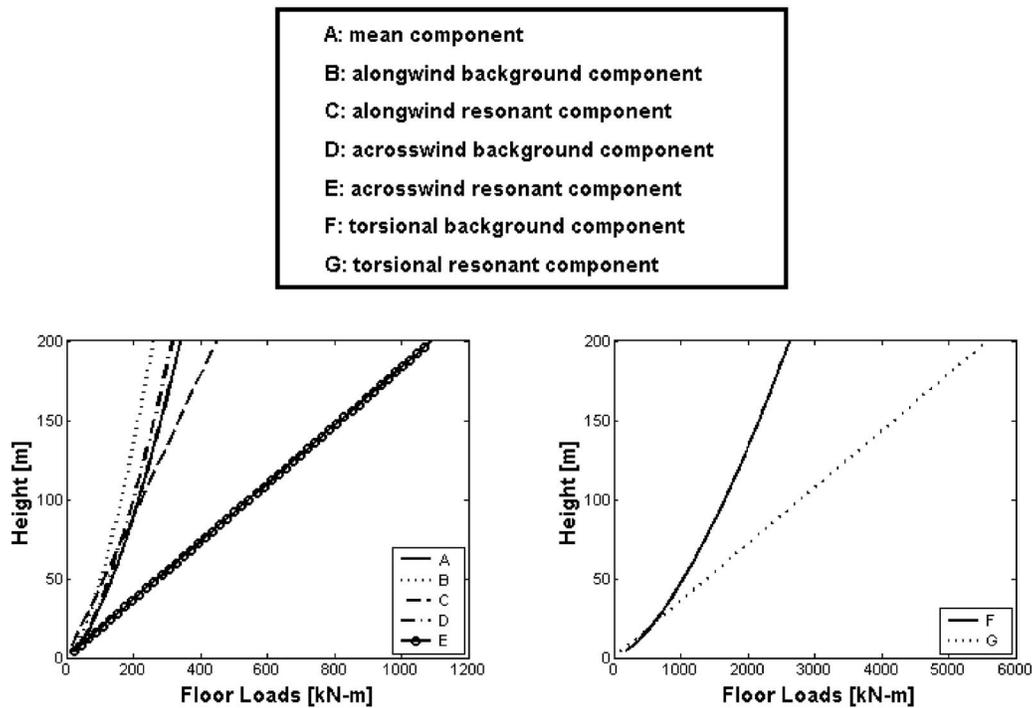
■ Download data file including all wind force components : w_force_all_ml00011.dat
(Column 1 : heights [*m*], Columns 2 to 8 : wind force component A to G [*kN, kN-m*])

Fig. 8. Display of on-the-fly calculated wind force components

only the PSD data offered by the NALD, but also any arbitrary PSD expression or data set for the on-line determination of wind load effects on high-rise buildings. Depending on the selected PSD option specified in Fig. 2, additional inputs will be requested following the prompt for structural inputs (interface 2 in Fig. 3). Fig. 10(a) shows the supplemental interface for user-supplied PSD expressions, while Fig. 10(b) shows the supplemental inter-face for user-supplied PSD data sets of X (reduced frequency) and Y (nondimensional base moment PSD) pairs. Since this on-line analysis module mainly utilizes MATLAB, the aforementioned inputs should be MATLAB compatible. The "info link" displayed in the top line provides the user with simple guidelines to mini-mize unexpected input errors. The on-line analysis module also includes a simple error-detection scheme with pop-up error mes-

Fig. 9. Diagram of NALD v. 2.0 architecture

□ Alongwind direction

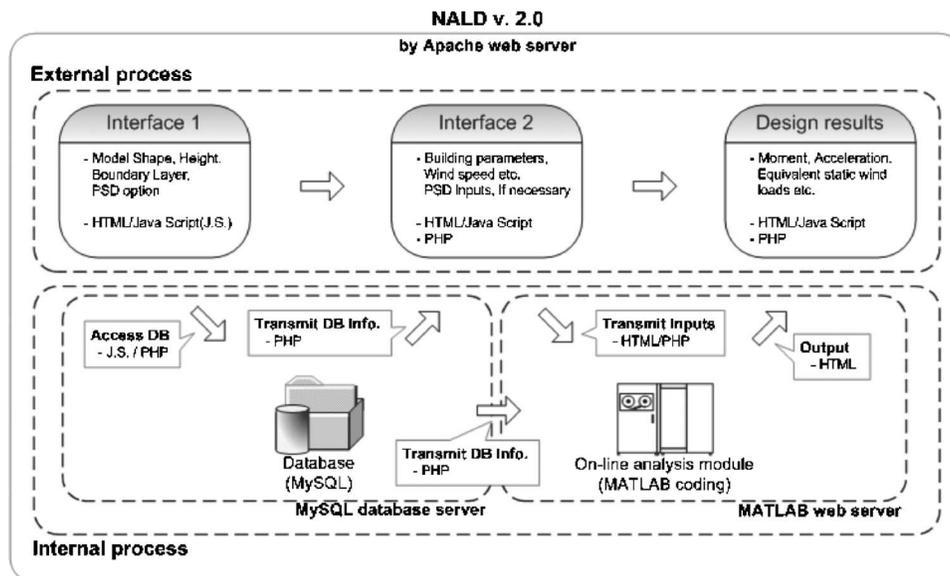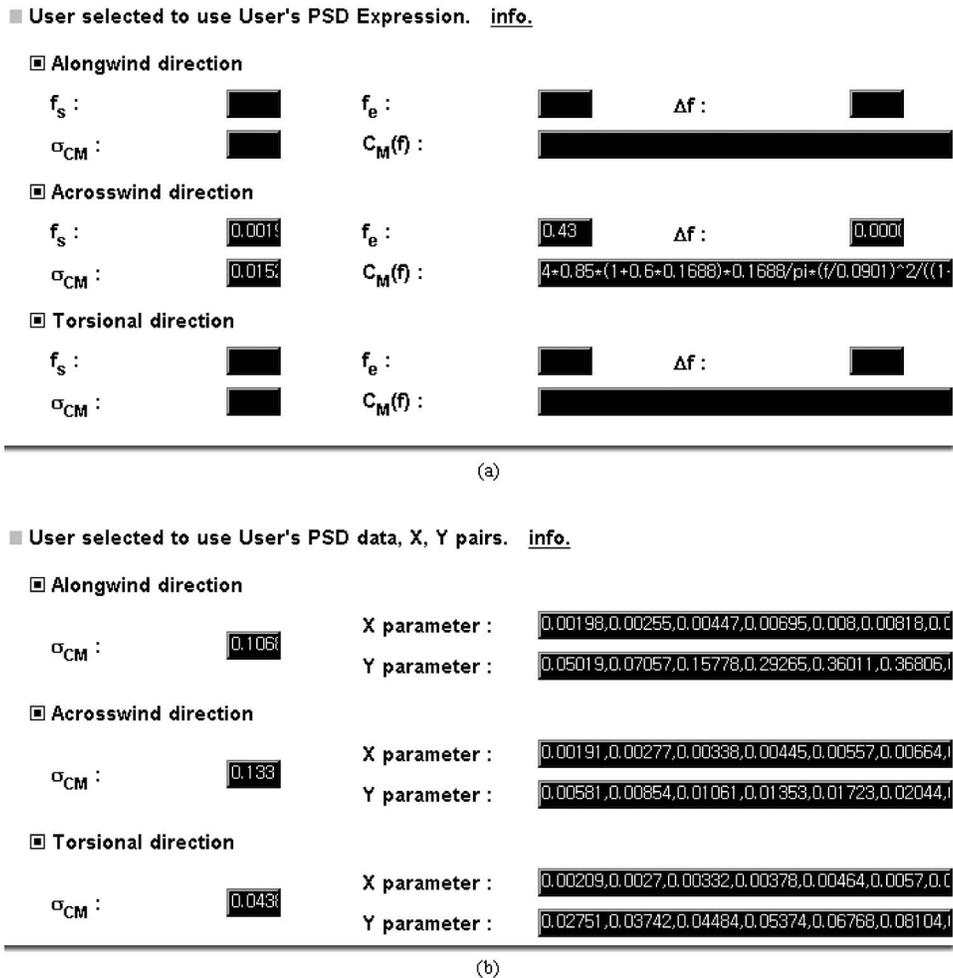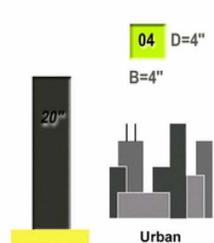f_s : [   ] f_e : [   ] Δf : [   ]

σ_{CM} : [   ] $C_M(f)$: [   ]

□ Acrosswind direction

f_s : [0.001] f_e : [0.43] Δf : [0.000]

σ_{CM} : [0.015] $C_M(f)$: [4*0.85*(1+0.6*0.1688)*0.1688/pi*(f/0.0901)^2/((1-]

□ Torsional direction

f_s : [   ] f_e : [   ] Δf : [   ]

σ_{CM} : [   ] $C_M(f)$: [   ]

(a)

□ Alongwind direction

σ_{CM} : [0.106]   X parameter : [0.00198,0.00255,0.00447,0.00695,0.008,0.00818,0.0]

Y parameter : [0.05019,0.07057,0.15778,0.29265,0.36011,0.36806,]

□ Acrosswind direction

σ_{CM} : [0.133]   X parameter : [0.00191,0.00277,0.00338,0.00445,0.00557,0.00664,]

Y parameter : [0.00581,0.00854,0.01061,0.01353,0.01723,0.02044,]

□ Torsional direction

σ_{CM} : [0.043]   X parameter : [0.00209,0.0027,0.00332,0.00378,0.00464,0.0057,0.0]

Y parameter : [0.02751,0.03742,0.04484,0.05374,0.06768,0.08104,]

(b)

Fig. 10. Supplemental interfaces for user-specified PSD with examples: (a) interface for PSD expression; (b) interface for PSD data

sages, which alert users if input values are beyond the NALD's range of applicability. The provision for PSD options extends the utility of NALD v. 2.0 beyond its predecessor by offering an on-line dynamic analysis framework that can be utilized for estimating dynamic load effects on high-rise buildings with alternative input options, e.g., an independent wind tunnel study or empirical expression from any wind load standard. This versatility provides users with a robust stand-alone, on-line analysis engine that offers the flexibility of utilizing user-supplied custom spectral description or wind tunnel test (HFBB) results to provide final design estimates of wind load effects on buildings and permit comparative studies of predictions from various sources.

Examples

The example building and wind environment used in Zhou et al. (2003) are utilized again in this study for consistency. Note that NALD v. 1.0 provided users with the spectral amplitude at a specified reduced frequency only; thus, it was required to perform manual calculation of the desired response components such as base moments and accelerations of building following the procedure provided on the NALD Web site (Zhou et al. 2003). The new version conducts all computations, including the ESWL calculations in all directions, automatically via the on-line analysis module. The example building characteristics are summarized here for

completeness and as a demonstration of the type of data an end user must input to analysis module: Building dimension perpendicular to oncoming wind $B=40$ m; building dimension parallel to oncoming wind $D=40$ m; building height $H=200$ m; natural frequency in alongwind, acrosswind, and torsional directions, respectively, $f_x=0.2$ Hz; $f_y=0.2$ Hz; $f_\theta=0.35$ Hz; bulk density $\rho_B=250$ kg/m³; average radius of gyration $\gamma=18$ m; damping ratio $\zeta=0.02$; interstory height $\Delta H=4$ m; air density $\rho_A=1.25$ kg/m³; drag force coefficient $C_D=1.3$; 3-sec reference wind speed at 10 m $U_{10}=63$ m/s (50-year MRI); mode shapes for all directions are assumed to be linear and the building is assumed to be located in an urban area. Thus, the NALD model best suited to this analysis is: Shape 4 ($D/B=1$), height=20 in. ($H/\sqrt{BD}=5$) in terrain category BL2 (Exposure A) (see Fig. 1). Based on these input conditions, analyses employing different PSD options are performed to demonstrate the capabilities of the on-line analysis module. An additional example (Example 4) is reported for a building used extensively in comparative studies and also in the Commentary for the Australian Standard (Holmes et al. 1990).

Example 1—NALD Experimental Data (PSD Option 1)

For the previously specified reference wind speed, the 50-year and 10-year wind speeds at the building height are determined to be 51.30 m/s and 37.96 m/s, respectively, for survivability and serviceability response estimates (Zhou et al. 2003). The corre-

Fig. 11. An example of error message for user-supplied inputs

sponding alongwind, acrosswind, and torsional loading spectra based on the NALD experimental data were shown previously in Fig. 6 and the display of the corresponding response estimates automatically computed by the on-line analysis module were previously demonstrated in Fig. 7. These include: Mean, peak background, peak resonant, and total peak base moments, and the maximum alongwind and acrosswind displacements at the roof level for survivability design, and peak and RMS accelerations at the roof level for serviceability design. The moment and acceleration values match those manually computed by Zhou et al. (2003). The output also includes distributions of the equivalent static wind load components: Mean, background, and resonant, for all response directions, as shown previously in Fig. 8. These load distributions can be downloaded by the user for incorporation into models developed using various commercial software packages to allow for further analysis and design of structural members. This exercise reaffirms that the real-time analysis module provides response estimates that are consistent with manual calculations presented previously by Zhou et al. (2003).

Example 2—User's PSD Expression (PSD Option 2)

As mentioned earlier, NALD v. 2.0 provides the user with an opportunity to utilize the various types of empirical PSD expressions available. This permits comparative analyses to demonstrate the impacts of generalized spectral expressions versus precise spectral values drawn directly from PSDs of HFBB data. In this example, acrosswind PSD expressions specified by AIJ (1996, 2004) and Gu and Quan (2004), detailed in the Appendix, are considered.

The requisite inputs for this option were shown previously in Fig. 10(a): $C_M(f)$, $S_M(f)$, σ_M, in a MATLAB compatible format, the reduced frequency range (f_s to f_e), reduced frequency interval (Δf), and σ_{CM}. If the user leaves blank(s) for any loading direction, the analysis will default to the NALD experimental data for that direction, and an error message will be displayed, as shown in Fig. 11. Based on the aforementioned example parameters, a comparison between the NALD v. 2.0 experimental PSD data and other two aforementioned empirical PSD expressions was shown in Fig. 12. It should be noted that AIJ (1996, 2004) empirical expressions are not a function of boundary layer condition, terrain category, and building height, but are expressed mainly as a function of the side ratio (D/B), whereas Gu and Quan (2004) incorporate the preceding attributes in their empirical expression (see the Appendix). This demonstrates a major drawback of empirical expressions: The need to incorporate an exhaustive set of variables in the expression in order to fully encompass various structural and flow features influencing response. Such considerations

were the motivating factors behind the on-line database approach represented by NALD v. 1.0. Despite the dependence on so many variables, the NALD result shows relatively good agreement with both empirical expressions with the exception of discrepancies in the low-frequency range, which are not of concern given the lack of their practical significance for typical high-rise buildings. Note also the high-frequency details lost in the empirical expressions.

To perform the on-line analysis, the reduced frequency range of the NALD experimental data is imposed on the two acrosswind PSD expressions, i.e., $f_s=0.0019$; $f_e=0.43$; $\Delta f=0.0001$. The RMS base bending moment coefficients (σ_{CM}) are automatically calculated from the respective empirical expressions (Appendix). For demonstrative purposes, the specifications of these empirical PSD expressions in a MATLAB compatible format are listed below:

AIJ (1996)

$$4 * 0.85 * (1 + 0.6 * 0.1688) * 0.1688/\text{pi} * (f/0.0901)^\wedge 2/$$

$$((1 - (f/0.0901)^\wedge 2)^\wedge 2 + 4 * 0.1688^\wedge 2 * (f/0.0901)^\wedge 2)$$

AIJ (2004)

$$4 * 0.85 * (1 + 0.6 * 0.2806) * 0.2806/\text{pi} * (f/0.0901)^\wedge 2/$$

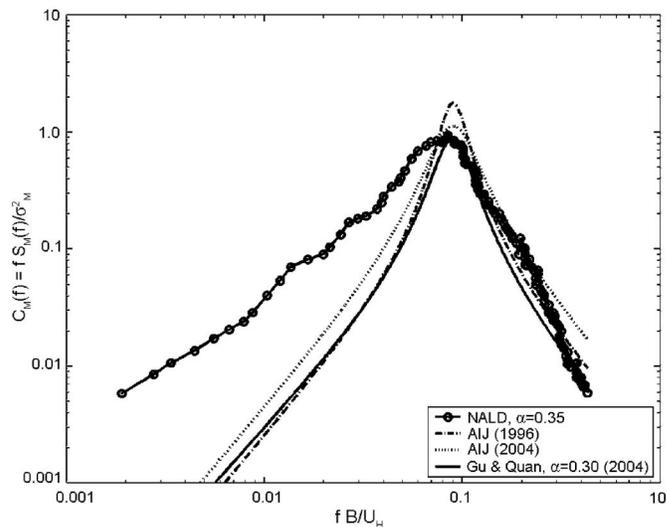$$((1 - (f/0.0901)^\wedge 2)^\wedge 2 + 4 * 0.2806^\wedge 2 * (f/0.0901)^\wedge 2)$$

Fig. 12. Comparison of acrosswind spectra with empirical expressions of AIJ (1996, 2004) and Gu and Quan (2004) ($D/B=1.0$, Exposure A)

Table 1. Acrosswind Analysis Results for Empirical PSD Expressions in Example 2 ($D/B=1.0, H/\sqrt{BD}=5$)

	σ_{CM}	RMS acceleration [mg]	Base bending moment [10^6 kN m]
NALD v. 2.0	0.1330	6.21	3.830
AIJ (1996)	0.1572	6.27	3.925
AIJ (2004)	0.1572	8.11	4.771
Gu and Quan (2004)	0.2122	7.34	4.692

Gu and Quan (2004)

$$1/0.2122^2 * (0.0396 * 0.1990 * (f/0.0897)^{1.8698})/$$

$$((1 - (f/0.0897)^2)^2 + 0.1990 * (f/0.0897)^2)$$

The resulting RMS base bending moment coefficient (σ_{CM}), total base moments (M_{total}), and RMS accelerations (a_{RMS}) derived from the four different PSDs [NALD default; user-specified AIJ (1996), AIJ (2004) and Gu and Quan (2004)] are summarized in Table 1. A quick review of the results suggests that those based on the NALD experimental data and AIJ (1996) compare well with one another. The same can be said for the results based on AIJ (2004) and Gu and Quan (2004), which take on slightly larger values than the former pair. It is important to note that RMS base bending moment coefficient (σ_{CM}) is quite sensitive to the approach flow characteristics. Thus, it becomes evident that reliable estimates of the RMS coefficient and the spectral amplitude are critical to the accurate evaluation of aerodynamic load information. Though empirical fits to experimental data, such as those in AIJ (1996, 2004), provide compact representations for use in codes and standards, they cannot accurately represent experimental data for all possible building configurations and flow conditions, again motivating the on-line database philosophy of NALD v. 2.0. However, in light of these factors, the results are in reasonable agreement. Furthermore, it is also demonstrated here that the on-line analysis module works effectively for user-supplied PSD expressions.

Example 3—User-Specified PSD Data (PSD Option 3)

Another PSD option offered by NALD v. 2.0 is the user-specified PSD data in the form of X, Y pairs. The prompt for this data allows the user to implement his/her own PSD data derived from a wind tunnel experiment. As shown previously in Fig. 10(b), three inputs are requested in each direction: RMS base bending moment coefficient (σ_{CM}), X coordinate [reduced frequency, $f \times B/U_H$], and Y coordinate (nondimensional power spectrum $C_M(f)$]. All X and Y input should be separated by a comma (,) or single space, and the total number of X values should be the same

Table 2. Design Results for Data from NALD v. 2.0 and Cheng and Wang (2004) ($D/B=1.0, H/\sqrt{BD}=5$)

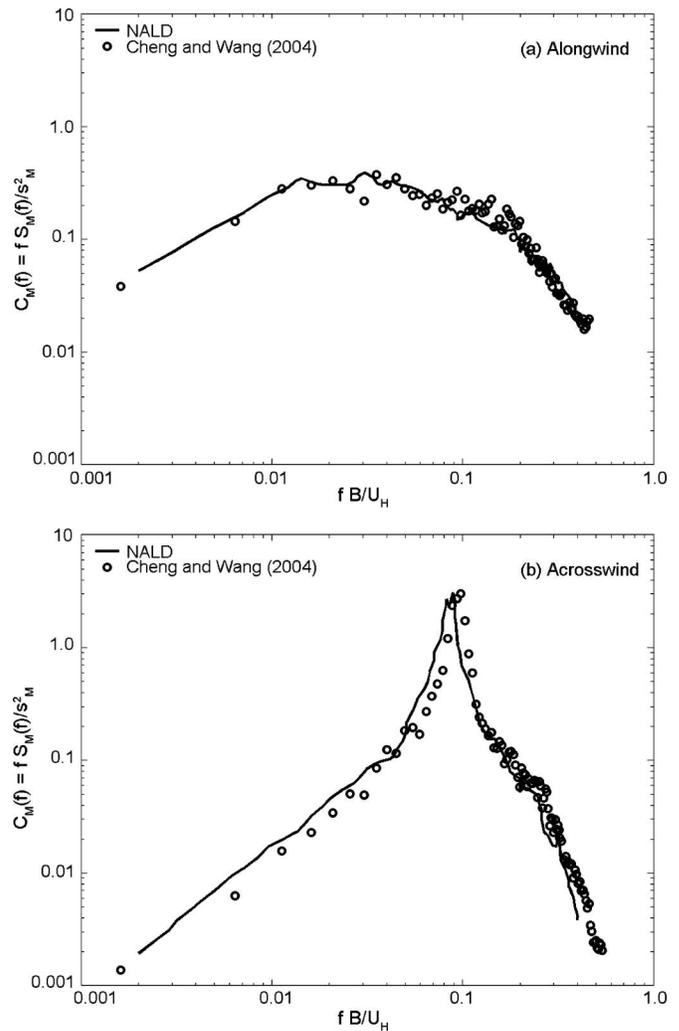|	Alongwind		Acrosswind	
	Base bending moment [10^6 kN m]	RMS acceleration [mg]	Base bending moment [10^6 kN m]	RMS acceleration [mg]
NALD v. 2.0	4.818	5.69	6.388	11.73
Cheng and Wang (2004)	5.158	6.29	6.639	11.17

Fig. 13. Comparison of alongwind and acrosswind between NALD and Cheng and Wang (2004) ($D/B=1.0, H/\sqrt{BD}=5$, Exposure C)

as Y values. Should the user inputs be in error, the user is alerted and NALD PSD data will be retrieved by default, as shown previously by the error pop up in Fig. 11.

Fig. 10(b) shows an example of this PSD option, using the download of one of the test cases archived in NALD v. 2.0. As expected, the results exactly replicate the results obtained using PSD option 1 (Example 1) and presented by Zhou et al. (2003) and, thus, are not repeated here. This demonstrates the accuracy of an on-line module in evaluating building response based on user-specified spectral data values. Another example utilizing the data by Cheng and Wang (2004) (PSD option 3) is also compared to the NALD experimental data for the case of $D/B=1.0, H/\sqrt{BD}=5$ under BL1 (Exposure C) for the alongwind and acrosswind directions. Table 2 summarizes the resulting base bending moments and RMS accelerations. Since the NALD spectra and Cheng and Wang (2004) data show a good agreement in the alongwind and acrosswind directions, as shown in Figs. 13(a and b), it is obvious that the response quantities correspondingly show a good agreement in Table 2.

These last two examples demonstrate the utility of the various PSD input options in this on-line analysis, providing the user with the versatility to perform an automated on-line analysis of wind

Table 3. Comparison of NALD v. 2.0 with AS 1170.2 and ASCE 7-05 for CAARC Building

		Responses	AS 1170.2	ASCE[a] exposure B	NALD v. 2.0		
					Average[b]	Exposure C	Exposure A
Case 1	Alongwind	Peak acceleration [mg]	8.24[c]	6.97	8.60	7.67	9.52
		Base moment [10^6 kN m]	2.80	2.42	2.31	2.16	2.46
	Acrosswind	Peak acceleration [mg]	15.53[c]	—[d]	11.52	11.22	11.81
		Base moment [10^6 kN m]	1.30	—[d]	1.47	1.11	1.83
Case 2	Alongwind	Peak acceleration [mg]	5.47[c]	4.65	5.88	5.07[e]	6.69[e]
		Base moment [10^6 kN m]	1.68	1.51	1.32	1.22	1.41
	Acrosswind	Peak acceleration [mg]	17.44[c]	—[d]	11.83	11.04[e]	12.62[e]
		Base moment [10^6 kN m]	1.89	—[d]	1.88	1.71	2.04

[a]ASCE 7-05 (ASCE 2005). Peak accelerations are calculated multiplying RMS acceleration by resonant peak factor and total moments are integrated wind loads determined by design wind pressure over full height of structure considering gust effect factor.

[b]It is obtained from taking averages of Exposures C and A results.

[c]Peak factor for 1 h is considered, instead of 10 min.

[d]ASCE only treats the alongwind direction.

[e]Extrapolated values, since ranges of reduced frequency are beyond acrosswind spectra.

effects on a high-rise building using his/her own data or an established expression for the base moment spectrum and evaluate various design options expediently.

Example 4—Comparison to Australian Standard

It is of interest to examine how the NALD v. 2.0 analysis compares with the dynamic response estimates of major building codes and standards. *A Commentary on the Australian Standard for Wind Loads* reported a detailed procedure for the dynamic analyses in the alongwind and acrosswind directions in Appendix C of that standard, using the Commonwealth Aeronautical Advisory Research Council (CAARC) standard tall building (Holmes et al. 1990). This CAARC building is analyzed by AS 1170.2, NALD v. 2.0, and ASCE 7-05 (ASCE 2005). The CAARC building's main characteristics are summarized here: Case 1. $B=46$ m; $D=30$ m; Case 2. $B=30$ m; $D=46$ m (Case 2 represents a 90 deg angle of incidence for the same building in Case 1); $H=183$ m; $f_x=f_y=0.2$ Hz; $\rho_B=160$ kg/m^3; $\zeta=0.015$ for serviceability design and 0.050 for survivability design; $C_D=1.3$ for Case 1 and 1.19 for Case 2; mode shapes for all directions are assumed linear. In Holmes et al. (1990), it was assumed that the CAARC building was located in Brisbane (terrain category 3), which corresponds to Exposure B in ASCE 7-05. Since NALD v. 2.0 handles Exposures A (BL2) and C (BL1) only, comparisons are made for both exposures, as well as their average, as they should provide upper and lower limits for the CAARC building. It should be pointed out that base moments in the AS 1170.2 were calculated for the ultimate limit state design, corresponding to wind speed of 1,000-year return period, while accelerations were

calculated for a 5-year return period, and the peak factor was evaluated for 10 min, instead of the 1-hour used in both NALD v. 2.0 and ASCE 7-05. On the other hand, NALD v. 2.0 observes the standards set by ASCE 7: 50-year return period for base moments (survivability design), and 10-year return period for accelerations (serviceability design). Thus, proper modifications to wind speed (to account for differences in return period) and peak factor (to account for differences in averaging interval) are required to compare AS 1170.2 with both NALD v. 2.0 and ASCE 7-05 results. As such, AS 1170.2 RMS results are translated to peak accelerations based on a peak factor calculated over 1 h. The design wind speed for NALD v. 2.0 and ASCE 7-05 are adjusted using the relationships in ASCE 7-05 for a 1,000-year return period in base moment calculations and a 5-year return period in acceleration calculations, so that they may be compared to the results of AS 1170.2 directly. As shown in Table 3, AS 1170.2 responses show relatively higher values (conservative) in comparison with NALD v. 2.0 and ASCE 7-05, except for the alongwind peak accelerations, which show good agreement. The discrepancies may in part be attributed to the measurement approach used to estimate aerodynamic loads. The data used in the Australian Standard are based on an aeroelastic model, and load spectra are estimated by an inverse approach, which may have inherent identification sensitivities. The other possible source may be the differences in the approach flow conditions, which have been observed to have notable influence on the acrosswind response. Another important advantage of NALD v. 2.0 is also underscored by this example; it provides a means to estimate the acrosswind response that ASCE 7 does not provide, outside of its commentary.

These examples demonstrate the capabilities and accuracy of NALD v. 2.0, providing a user-friendly procedure to reliably estimate building dynamic responses. The writers envision this capability to be particularly useful for those who may not be very familiar with the details of the dynamic analysis procedure typically employed in response estimation for wind-sensitive structures. In addition, the robust framework presented here is conveniently amenable to including additional data for other building cross sections and flow conditions.

Concluding Remarks

The rapid development of information technologies has revolutionized many engineering applications. This study discusses the use of these advances to enhance, for the purposes of analysis and design, the accessibility, organization, dissemination, and utility of wind tunnel data. The second version of the NatHaz Aerodynamic Loads Database (NALD v. 2.0) (http://aerodata.ce.nd.edu) integrates these technologies for the purpose of wind-induced response prediction. NALD v. 2.0 offers more attractive and user-friendly features to allow on-line determination of not only the base moments, displacements, and the equivalent static wind loads for survivability design, but also accelerations for serviceability (habitability) design. Several Web-based tools such as PHP and MySQL are fused with MATLAB to create efficient yet computationally robust interfaces that process, convert, and analyze wind tunnel data on-the-fly with minimal user effort. The attractive feature of this on-line processing approach is that no user intervention is expended in the determination and display of wind loads and response quantities for the preliminary design of high-rise buildings. Moreover, this on-line analysis module provides the flexibility to utilize not only the NALD experimental PSD data, but also user-specified PSD expressions or data sets. This versatility provides users with a robust stand-alone, on-line analysis engine for high-rise buildings using various data sources. Further, the architecture used in this study permits easy extensions to more sophisticated numerical analyses by employing the many predefined function capabilities of MATLAB operating on the server side. While, the analysis capabilities offered by NALD v. 2.0 are not necessarily intended to replace customized wind tunnel testing in the final design stages, they do provide users with an efficient means to approximate the complete 3D response of buildings in the early design stage, which has not been fully treated in most codes and standards. Additionally, the analysis engine built into NALD v. 2.0 offers the option of utilizing user-supplied custom spectral description or wind tunnel test results to obtain final design estimates of wind load effects on buildings.

It should be noted that the Web-based tools used to establish the interface and analysis modules described in this study are continuously updated as evolving security and vulnerability issues are identified. Due to this constant updating, the interfaces are likely to experience some cosmetic changes since the publication of this manuscript.

Acknowledgments

Appendix. Acrosswind PSD Expressions Used in Example 3

- AIJ Recommendations for Loads on Buildings (1996, 2004)

$$C_M(f) = \frac{f \times S_M(f)}{\sigma_M^2}$$

$$= \sum_{j=1}^{N} \frac{4K_j(1+0.6\beta_j)\beta_j}{\pi} \frac{(n_0/n_{sj})^2}{\{1-(n_0/n_{sj})^2\}^2 + 4\beta_j^2(n_0/n_{sj})^2}$$

where

$$N = \begin{cases} 1, & D/B < 3 \\ 2, & D/B \geq 3 \end{cases} \quad K_1 \approx 0.85 \quad K_2 \approx 0.02$$

$$n_0 = \frac{f \times B}{U_H} \quad n_{s1} = \frac{0.12}{\{1+0.38(D/B)^2\}^{0.89}} \quad n_{s2} = \frac{0.56}{(D/B)^{0.85}}$$

$$\beta_1 = \frac{(D/B)^4}{1.2(D/B)^4 - 1.7(D/B)^2 + 21} + \frac{0.12}{(D/B)} \quad \text{(AIJ 1996)}$$

$$\beta_1 = \frac{(D/B)^4 + 2.3(D/B)^2}{2.4(D/B)^4 - 9.2(D/B)^3 + 18(D/B)^2 + 9.5(D/B) - 0.15} + \frac{0.12}{(D/B)} \quad \text{(AIJ 2004)}$$

$$\beta_2 = 0.28(D/B)^{-0.34}$$

$$\sigma_{CM} = 0.0082(D/B)^3 - 0.071(D/B)^2 + 0.22(D/B)$$

- Gu and Quan (2004)

$$C_M(f) = \frac{f \times S_M(f)}{\sigma_M^2} = \frac{1}{\sigma_{CM}^2} \times \frac{S_p\beta(n_0/f_p)^\alpha}{\{1-(n_0/f_p)^2\}^2 + \beta(n_0/f_p)^2}$$

where

$$n_0 = fB/U_H$$

$$f_p = 10^{-5}(191 - 9.48\alpha_w + 1.28\alpha_{hr} + \alpha_{hr}\alpha_w)(68 - 21\alpha_{db} + 3\alpha_{db}^2)$$

$$S_p = (0.1\alpha_w^{-0.4} - 0.0004e^{\alpha_w})(0.84\alpha_{hr} - 2.12 - 0.05\alpha_{hr}^2)$$
$$\times (0.422 + \alpha_{db}^{-1} - 0.08\alpha_{db}^{-2})$$

$$\beta = (1 + 0.00473e^{1.7\alpha_w})(0.065 + e^{1.26-0.63\alpha_{hr}})e^{1.7-3.44/\alpha_{db}}$$

$$\alpha = (-0.8 + 0.06\alpha_w + 0.0007e^{\alpha_w})(-\alpha_{hr}^{0.34} + 0.00006e^{\alpha_{hr}})$$
$$\times (0.414\alpha_{db} + 1.67\alpha_w^{-1.23})$$

$$\alpha_w = 1(A), \ 2(B), \ 3(C), \ 4(D) \quad A,B,C,D : \text{Terrain categories}$$

$$\alpha_{hr} = H/\sqrt{BD}$$

$$\alpha_{db} = D/B$$

$$\alpha_{ht} = H/T \quad [T = \min(B,D)]$$

$$\sigma_{CM} = (0.002\alpha_w^2 - 0.017\alpha_w - 1.4)(0.056\alpha_{db}^2 - 0.16\alpha_{db} + 0.03)$$
$$\times (0.03\alpha_{ht}^2 - 0.622\alpha_{ht} + 4.357)$$

References

Architectural Institute of Japan (AIJ). (1996). "Recommendations for loads on buildings." Architectural Institute of Japan.

Architectural Institute of Japan (AIJ). (2004). "Recommendations for loads on buildings." Architectural Institute of Japan.

American Society of Civil Engineers (ASCE). (1998). "Minimum design loads for buildings and other structures." *ASCE 7-98*, ASCE, Reston, Va.

American Society of Civil Engineers (ASCE). (2005). "Minimum design loads for buildings and other structures." *ASCE 7-05*, ASCE, Reston, Va.

Boggs, D. W., and Peterka, J. A. (1989). "Aerodynamic model tests of tall buildings." *J. Eng. Mech.*, 115(3), 618–635.

Chan, C.-M., and Chui, J. K. L. (2006). "Wind-induced response and serviceability design optimization of tall steel buildings." *Eng. Struct.*, 28(4), 503–513.

Chen, X., and Kareem, A. (2004). "Equivalent static wind loads on buildings: New model." *J. Struct. Eng.*, 130(10), 1425–1435.

Chen, X., and Kareem, A. (2005). "Dynamic wind effects on buildings with 3-D coupled modes: Application of high frequency force balance measurements." *J. Eng. Mech.*, 131(11), 1115–1125.

Cheng, C.-M., and Wang, J. (2004). "Wind tunnel database for an intermediate wind resistance design of tall buildings." *Proc., 1st Int. Symp. on Wind Effects on Buildings and Urban Environment*, 10–25.

Davenport, A. G. (1967). "Gust loading factors." *J. Struct. Div.*, 93(3), 11–34.

Flay, R. G. J., and Bhat, J. (2005). "Cross-wind force spectra for building geometries commonly proposed for New Zealand cities." *Proc., 2nd Workshop on Regional Harmonization of Wind Loading and Wind Environmental Specifications in Asia-Pacific Economies (APEC-WW)*, 19–30.

Fritz, W. P., and Simiu, E. (2005). "Probabilistic description of tall building response to wind: Database-assisted design, dynamics, and wind directionality effects." *Proc., 9th Int. Conf. on Structural Safety and Reliability* (CD-ROM).

Fujii, K., Hibi, K., and Ueda, H. (1986). "A new measuring system using electronically scanned pressure sensors (ESP) and some applications of the ESP system to a square building shape." *Proc., 9th National Symp. on Wind Engineering*, 313–318 (in Japanese).

Gu, M., and Quan, Y. (2004). "Across-wind loads of typical tall buildings." *J. Wind. Eng. Ind. Aerodyn.*, 92(13), 1147–1165.

Ha, Y. C., Kim, D. W., and Kil, Y. S. (2004). "Characteristics of the across-wind fluctuating force and spectral density of rectangular high-rise buildings with various side ratios." *Proc., CTBUH 2004*, 978–982.

Ho, T. C. E., Lythe, G. R., and Isyumov, N. (1999). "Structural loads and responses from the integration of instantaneous pressures." *Wind Engineering into the 21st Century: Proc., 10th Int. Conf. on Wind Engineering*, A. Larsen, G. L. Larose, F. M. Livesey, eds., Balkema, Rotterdam, The Netherlands, 1505–1510.

Holmes, J. D., Melbourne, W. H., and Walker, G. R. (1990). "A commentary on the Australian standard for wind loads: AS 1170 part 2." Australian Wind Engineering Society.

Holmes, J. D., Rofail, A. W., and Aurelius, L. J. (2003). "High frequency base balance methodologies for tall buildings with torsional and coupled resonant modes." *Proc., 11th Int. Conf. on Wind Engineering*, 2381–2388.

Huang, G., and Chen, X. (2007). "Wind load effects and equivalent static wind loads of tall buildings based on synchronous pressure measurements." *Eng. Struct.*, 29(11) 2641–2653.

Kareem, A. (1982). "Fluctuating wind loads on buildings." *J. Engrg. Mech. Div.*, 108(6), 1086–1102.

Kareem, A. (1990). "Measurement of pressure and force fields on building models in simulated atmospheric flows." *J. Wind. Eng. Ind. Aerodyn.*, 36(1), 589–599.

Kareem, A., and Cermak, J. E. (1979). "Wind tunnel simulation of wind-structure interactions." *ISA Trans.*, 18(4), 23–41.

Kareem, A., and Zhou, Y. (2003). "Gust loading factor—Past, present and future." *J. Wind. Eng. Ind. Aerodyn.*, 91(12–15), 1301–1328.

Kijewski, T., and Kareem, A. (1998). "Dynamic wind effects: A comparative study of provisions in codes and standards with wind tunnel data." *Wind Struct.*, 1(1), 77–109.

Kijewski, T., Kwon, D., and Kareem, A. (2003). "e-technologies for wind effects on structures." *Proc., 11th Int. Conf. on Wind Engineering*, 2217–2224.

Kikuchi, H., Tamura, Y., Ueda, H., and Hibi, K. (1997). "Dynamic wind pressures acting on a tall building model—Proper orthogonal decomposition." *J. Wind. Eng. Ind. Aerodyn.*, 69–71, 631–646.

Kwon, D., Kijewski-Correa, T., and Kareem, A. (2005). "e-analysis/design of tall buildings subjected to wind loads." *Proc., 10th Americas Conf. on Wind Engineering* (CD-ROM), Paper No. 123, AAWE.

Liang, S., Li, Q. S., Liu, S., Zhang, L., and Gu, M. (2004). "Torsional dynamic wind loads on rectangular tall buildings." *Eng. Struct.*, 26(1), 129–137.

Liang, S., Liu, S., Li, Q. S., Zhang, L., and Gu, M. (2002). "Mathematical model of acrosswind dynamic loads on rectangular tall buildings." *J. Wind. Eng. Ind. Aerodyn.*, 90(12–15), 1757–1770.

Lin, N., Letchford, C., Tamura, Y., Liang, B., and Nakamura, O. (2005). "Characteristics of wind forces acting on tall buildings." *J. Wind. Eng. Ind. Aerodyn.*, 93(3), 217–242.

McNamara, R. J. (2005). "Some current trends in high rise structural design." *Structure Magazine*, September, 19–23.

Reinhold, T. A., and Kareem, A. (1986). "Wind loads and building response predictions using force-balance techniques." *Proc., 3rd ASCE Engineering Mechanics Specialty Conf. on Dynamic Response of Structures*, ASCE, New York, 390–397.

Solari, G., and Kareem, A. (1998). "On the formulation of ASCE 7-95 gust effect factor." *J. Wind. Eng. Ind. Aerodyn.*, 77–78, 673–684.

Steckley, A., Accardo, M., Gamble, S. L., and Irwin, P. A. (1992). "The use of integrated pressures to determine overall wind-induced response." *J. Wind. Eng. Ind. Aerodyn.*, 42(1–3), 1023–1034.

Tamura, Y., Kareem, A., Solari, G., Kwok, K. C. S., and Holmes, J. D. (2005). "Aspects of the dynamic wind-induced response of structures and codification." *Wind Struct.*, 8(4), 251–268.

Tamura, Y., Kawai, H., Uematsu, Y., Marukawa, H., Fujii, K., and Taniike, Y. (1996). "Wind load and wind-induced response estimations in the 'Recommendations for loads on buildings,' AIJ 1993." *Eng. Struct.*, 18(6), 399–411.

Tschanz, T., and Davenport, A. G. (1983). "The base balance technique for the determination of dynamic wind loads." *J. Wind. Eng. Ind. Aerodyn.*, 13(1–3), 429–439.

Vickery, P. J., Steckley, A. C., Isyumov, N., and Vickery, B. J. (1985). "The effect of mode shape on the wind-induced response of tall buildings." *Proc., 5th U. S. National Conf. on Wind Engineering*, Vol. 1B, 41–48.

Xu, Y. L., and Kwok, K. C. S. (1993). "Mode shape corrections for wind tunnel tests of tall buildings." *Eng. Struct.*, 15(5), 387–392.

Zhou, Y., and Kareem, A. (2001). "Gust loading factors: New model." *J. Struct. Eng.*, 127(2), 168–175.

Zhou, Y., Kareem, A., and Gu, M. (2002). "Mode shape corrections for wind load effects." *J. Eng. Mech.*, 128(1), 15–23.

Zhou, Y., Kijewski, T., and Kareem, A. (2003). "Aerodynamic loads on tall buildings: Interactive database." *J. Eng. Mech.*, 129(3), 394–404.